D. ANTONY PRABU©[1*], K.S. JAYAKUMAR©[2], E. MADHAVAN PILLAI©[1], G. KUMARESAN©[3]

OPTIMIZATION OF GTAW PROCESS PARAMETERS OF DISSIMILAR Al-Mg ALLOYS FOR ENHANCED JOINT STRENGTH – TAGUCHI APPROACH

The Tungsten Inert Gas (TIG) welding processes one of the prevalent methods used for welding aluminum alloys. TIG welding is most commonly used due to its superiority in welding less dense materials. The most prevalent issues encountered with TIG welding aluminium alloys are porosity creation and cracking due to solidification, both of which result in lower mechanical properties. Because of the metal's susceptibility to heat input, this occurs. The current work is the result of a desire to improve the mechanical properties of dissimilar aluminium metals: AA5052-H32 & AA5083-H111. The process parameters of TIG welding are optimized towards eliminating the previously discussed failure scenarios. Various optimization techniques exist towards obtaining optimizing processes such as Response Surface Methodology (RSM), Genetic Algorithm (GA), Artificial Neutral Network (ANN), Flower pollination algorithm, Taguchi method etc, The Taguchi method was chosen for the optimization of process parameters due to its inherent nature of solving problems of singular variance. The optimal parameters combination was determined i.e. welding current at 170 A, filler rod diameter 2.4 mm and Gas flow rate of 11 lpm. The optimized input parameter was used to TIG weld the confirmation specimen which are further investigated for mechanical and metallurgical characterizations. The parameters were optimized and the results indicate that the input current was found to be the most contributing towards improving mechanical properties over all the process parameters.

Keywords: AA5052-H32; AA5083-H111; Mechanical properties; Microstructures; Optimization; Tungsten Inert gas welding

1. Introduction

Aluminum (Al)-Magnesium (Mg) based alloys such as AA5083, AA5052 [1] have recently been widely used in sophisticated structural engineering (aerospace, marine) applications. These alloys offer exceptional mechanical and corrosion properties, as well as being cost effective [2]. Because Al-Mg based alloys have a high vaporisation element, they are not suited for conventional fusion welding methods [3-4]. The current work investigates the aluminium alloys AA5053-H32 and AA5083-H111 as base metals for TIG welding process parameter improvement. In marine and chemical environments, AA5052 in H32 temper offers excellent corrosion resistance [5]. The alloy has good weldability and cold formability. It has a medium to high strength as well as comparable fatigue strength [6]. AA5083 grade aluminum alloys have trace amounts of manganese and chromium alloyed with magnesium which make them highly resistant to attack by seawater and industrial chemicals [7] "Which are particularly capable of retaining high degree of strength after

welding. Gas Tungsten arc welding (GTAW) also called as Tungsten Inert Gas (TIG) welding is the method often preferred over Metal Inert Gas (MIG) welding nowadays" [8-10]. This is due to the fact that TIG welding allow for better results in welding of lighter gauge metals [11]. "Under optimized circumstances TIG welding could possibly produce high quality welds. There are many TIG input process parameters that influence the mechanical properties of the welded joint such as welding current, voltage, welding speed, gas flow rate and dimensions of the welding filler rod" [12]. "The fine grain structures resulting from an optimum weld are capable of producing better mechanical properties such as higher tensile strength, improved hardness and high impact resistance of the welded joint" [13-14]. "Generally, TIG welding process consists of four different welded regions namely 1. Weld Zone (WZ), 2. Heat Affected Zone (HAZ) and 3. Base Metal (BM). Various optimization techniques such as Analysis of Variance, Taguchi, Response Surface Methodology (RSM), Genetic algorithm (GA), Artificial Neutral Network (ANN) etc., can be used for optimization of welding processes. This study

1 LOYOLA-ICAM COLLEGE OF ENGINEERING AND TECHNOLOGY (LICET), DEPARTMENT OF MECHANICAL ENGINEERING, LOYOLA CAMPUS, CHENNAI, TAMIL NADU, INDIA
2 SRI SIVASUBRAMANIYA NADAR COLLEGE OF ENGINEERING, DEPARTMENT OF MECHANICAL ENGINEERING, CHENNAI, TAMIL NADU, INDIA
3 BANNARI AMMAN INSTITUTE OF TECHNOLOGY, DEPARTMENT OF MECHANICAL ENGINEERING, SATHYAMANGALAM, ERODE, TAMIL NADU, INDIA

* Corresponding author: antonydprabu@gmail.com

uses Taguchi analysis due to its inherent efficiency in solving problems of single objective nature. The optimization of Taguchi analysis considers the three major design concepts or 1. System design, 2. Welding process design, and 3. Tolerance design" [15].

The entire analysis is broken down as follows:

Step 1 – Finding and optimizing the quality characteristic,

Step 2 – Pre-determining the noise factor and test conditions,

Step 3 – Pre-determining the factors and Levels,

Step 4 – Development of DOE (Design of Experiments),

Step 5 – Conduction of experiment based on DOE.

Step 6 – Analysis of input and output responses of optimum level for controlled factors

The present work investigates the mechanical performance and optimum TIG welding process parameters for AA5053-H32 and AA5083-H111 joint by using orthogonal array (OA). Three Levels and three factors L9 OA method was used. Furthermore, ANOVA statistical techniques are used to develop the mathematical relationship and to find the error percentage of actual and predicted values.

2. Methodology

Fig. 1 depicts the systematic approach used to determine the optimal TIG welding process parameters based on the welded parts' tensile strength and hardness (Hv). TABLE 1 shows the TIG welding input process parameters. Fig. 2(b) shows the TIG welded specimens under the process parameters of TABLE 1. The plates to be welded are milled to the requisite dimensions, which are 150×55×5 mm as indicated in Fig. 2c. The 45-degree taper is applied to the base plates at the plate's budding point. DOE was used to determine the number of trials. There were
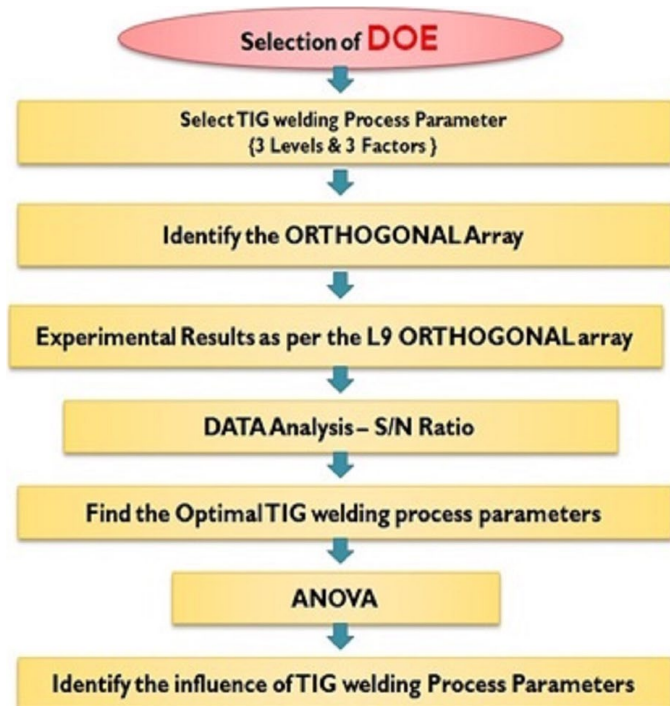
three stages and three factor designs to consider. The L9 orthogonal array was used to investigate TIG process parameters and determine the best settings based on weld joint mechanical properties. TABLE 2 provides the number of experiments as well as the mechanical parameters of each trail. Metallurgical studies such as Optical Microscopy (OM) and Scanning Electron Microscopy (SEM) are used to characterise optimised welded specimens (SEM).To explore the influence of TIG welded joints, microstructural investigations were conducted to find the distinct zones in TIG welded joints such as HAZ and WZ.
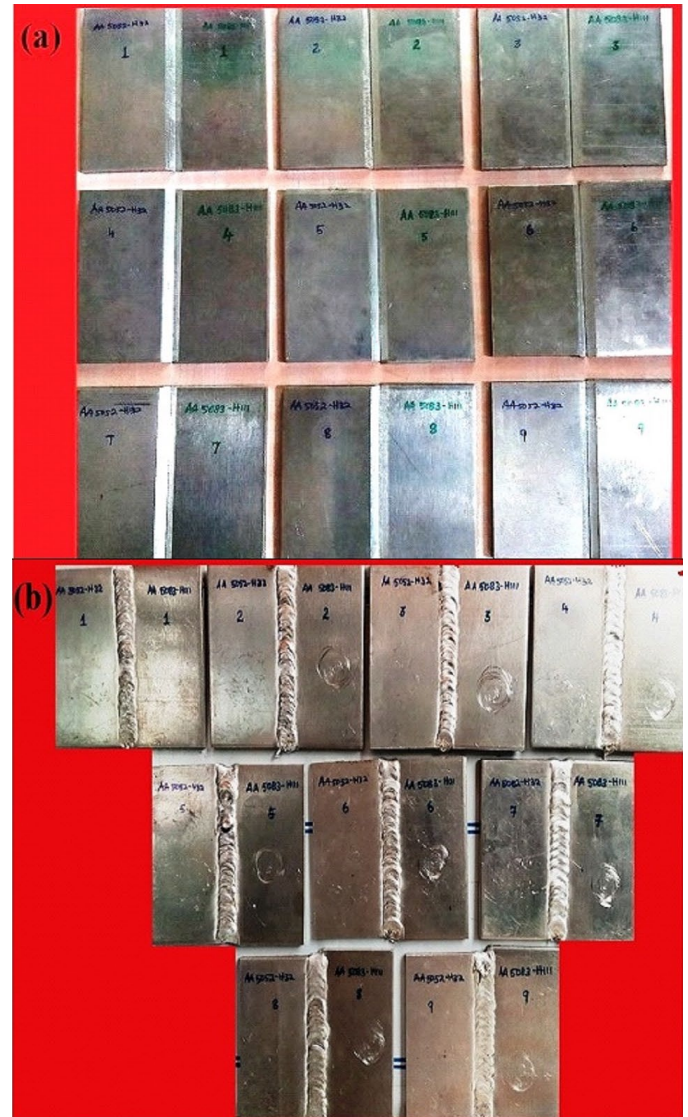

Fig. 2. (a) 9 samples of AA5052-AA5083 plates before welding (b) TIG welded AA5052-AA5083 dissimilar alloy specimens (c) Base plate with dimensional specifications

Fig. 1. Scheme of approach for process parameter optimization

TABLE 1

TIG weld Input Process parameter (3 levels and 3 factors)

S. No	Parameters	Levels		
		1	2	3
1	Current	150	170	190
2	Gas Flow Rate	10	11	12
3	Filler Rod Diameter	1.6	2	2.4

Level	Current	Gas flow rate	Filler rod diameter
1	40.50	40.72	37.99
2	42.21	41.00	41.94
3	39.82	40.80	42.58
Delta	2.39	0.27	4.59
Rank	2	3	1

3. Mechanical behavior of welded samples

3.1. Tensile test

A universal tensile testing machine was used to determine the ultimate tensile strength and amount of elongation of the welded specimens. The test specimens for the tensile test were produced in accordance with the ASTM E08 standard. A wire cut machine was used to create the tensile test specimens. Before testing, ASTM E8M04 standard sized tensile test specimens of TIG welded AA5052-AA5083 are shown in Fig. 3(a). The test was performed at ordinary room temperature with a strain rate of 5 mm/min. Fig. 3 depicts the shattered specimens (b).

3.2. Vickers microhardness test

To determine the microhardness of the welded AA5052-AA5083 junction, the Vickers hardness test was used. The findings of the TIG welded joints' hardness study are shown in TABLE 2. The hardness profile of the AA5052-AA5083 joint was analyzed by using Shimadzu HMV-2 Digital Micro-Hardness Tester machine. The hardness was analyzed on different zones of the weldments such as WZ, HAZ and the base metal. Mechanical polishing and Keller's agent were used to prepare the surface of the welded specimens according to ASTM standards. The dwell time used was 15 s for each specimen. The diamond indenter was used to apply a load of 500 g for the reported dwell time. The Vickers microhardness of the weld zone, heat impacted zone, and base metals surface were calculated using formulaic calculations using the indent and area of indentation.

3.3. Charpy Impact test

The usual Charpy V-notch impact testing approach was utilised to study the specimen's impact resistance behaviour as well as the toughness of the weld junction. The test was carried out to investigate the shock loading mechanics and their impact on the specimen's energy absorption and fracture behaviour. The specimens were made to conventional measurements of 55×10 mm with a 2 mm deep v-notch. On one face, the specimens were produced with a tip radius of 0.25 mm. Fig. 4(a) represents the impact test specimens prior to analysis, while Fig. 4(b) depicts the impact test samples after analysis.

4. Results and discussion

4.1. Analysis of results- Taguchi

To get the optimal parametric values for TIG welding of the AA5052-AA5083 joint, the Taguchi method was employed for optimization analysis of the process parameters. The Signal-to-Noise (S/N) ratio is a statistical performance assessment used in this procedure. Because it is a logarithmic function, the S/N ratio is the optimization's objective function. The signal-to-noise
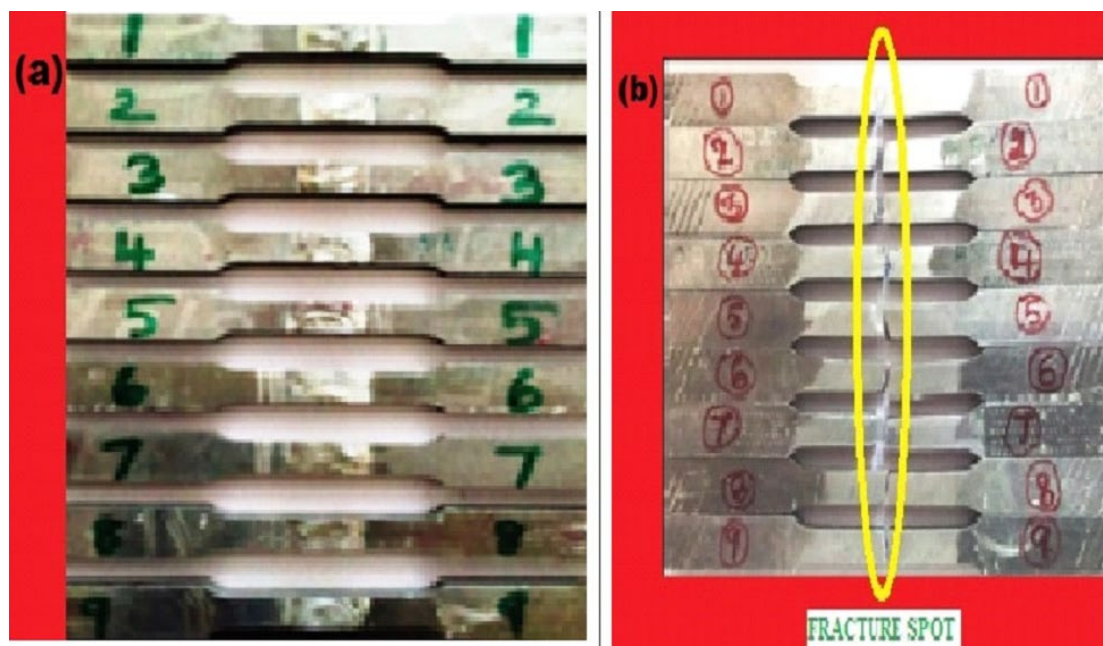

Fig. 3. (a) Tensile test specimens before tensile test; (b) Fractured tensile specimens after test
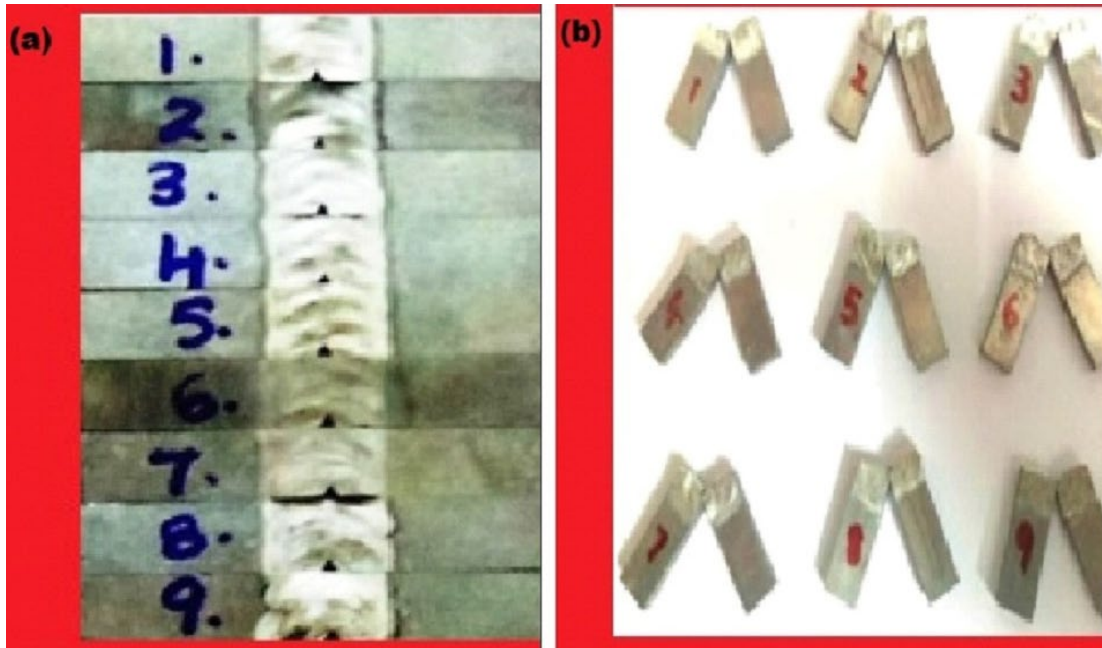
Fig. 4. (a) Charpy impact test specimens before testing (b) Charpy impact test specimens after testing

ratio is the ratio of the signals (mean) to the noise (standard deviation). This ratio is used to identify the factors that control the variability in a sample environment. The ratios are generally measured for performance as either 'Lower the Better' or in the case of the present work, 'Larger the Better'. The results of the analyses are tabulated and illustrated in TABLES 2-4 and Figs 6-8 respectively.
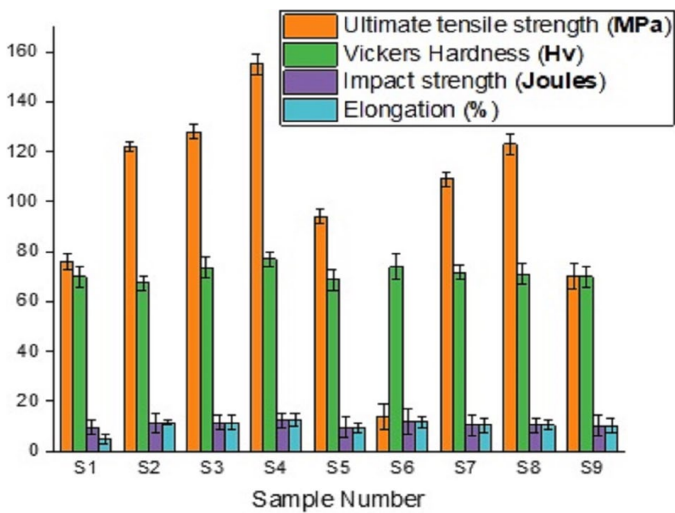

Fig. 5. Experimental results – Mechanical Properties of TIG welded joints

The optimized values obtained for the process parameters for improved ultimate tensile strength can be inferred form TABLE 2. The impacts of process factors on tensile strength for S/N ratios are shown in Fig. 6. The S/N ratio peaks at 170A at 42.21. The peak S/N ratio obtained for the gas flow rate is 40.72 at 11 lpm. Similarly the peak S/N ratio of 42.58 is obtained when filler rod diameter is 2.4 mm. These peak values signify

the optimum value of TIG welding parameters for obtaining maximum ultimate tensile strength. The resultant values have been show in Fig. 5 for inference.
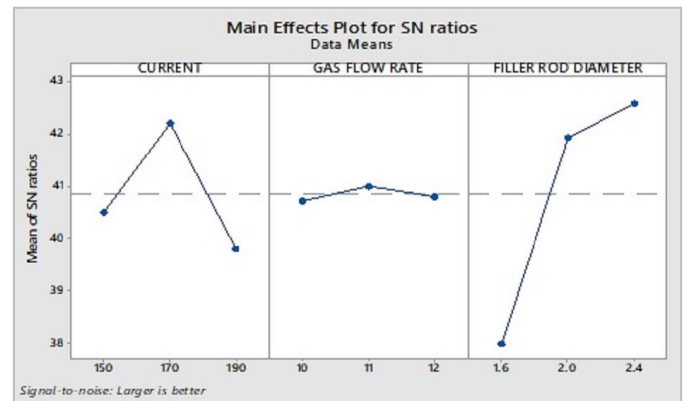

Fig. 6. Effects of process parameters on S/N ratios for ultimate tensile strength

The optimized values obtained for the process parameters for improved microhardness can be inferred form TABLE 3. The table offers the response values for S/N ratios for microhardness under the varied process parameter values and Fig. 6 illustrates the trend of the S/N ratio affected by these process parameters. As can be observed, the maximum S/N ratio of 37.29 is obtained for input current of 170 A. The S/N ratio is less than the said value when the input current is at 160 A or 180 A. The peak S/N ratio value is obtained when the gas flow rate is 10 lpm. The S/N ratio value obtained is 37.24 which are higher than those obtained when the flow rate is 11 lpm and 12 lpm. The S/N ratio is progressive when the filler rod diameter is increased. Peak S/N ratio is obtained when the filler rod diameter is also at peak input of 2.4 mm; the S/N ratio obtained is 37.37.

TABLE 3

Response Table for Signal to Noise Ratios (Larger is better)
– Microhardness

Level	Current	Gas flow rate	Filler rod diameter
1	36.93	37.24	36.84
2	37.29	36.78	37.02
3	37.01	37.21	37.37
Delta	0.35	0.46	0.52
Rank	3	2	1

The S/N ratios found for optimizing Impact resistance under the TIG welding process parameters of current, gas flow rate, and filler rod diameter are listed in TABLE 4. Fig. 7 illustrates that the peak S/N ratio for the TIG process parameter current is 21.01 at 170A, with the S/N ratio dropping below 21 under 150A and 190A current input. The S/N ratio is 20.65 when gas flow rate is 10 lpm and drops to 20.40 at 11 lpm but rises to peak value of 20.99 when gas flow rate is 12 lpm. The plot also illustrates that the S/N ratio begins at 19.88 at 1.6 mm filler rod diameter and rises sharply to peak value of 21.17 when the filler rod diameter is 2.4 mm.

TABLE 4

Response Table for Signal to Noise Ratios (Larger is better)
– Impact resistance

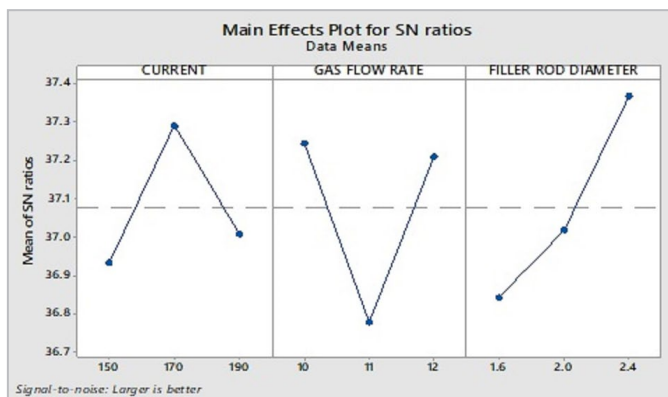| Level	Current	Gas Flow Rate	Filler Rod Diameter
1	20.70	20.65	19.88
2	21.01	20.40	21.00
3	20.34	20.99	21.17
Delta	0.67	0.59	1.29
Rank	2	3	1

Fig. 7. Effects of process parameters on S/N ratios for Microhardness

Based on quality characteristic the significant TIG welding process parameters were identified by using ANOVA. This method is also used to discover the best TIG welding parameters based on the output responses of TIG welded joints' tensile strength and hardness. The signal-to-noise (S/ N) ratio is used to calculate the error percentage and determine the influence and contribution of each TIG welding process parameter. Eq. (1) shows the S/N ratio based on Taguchi method and Eq. (2) shows

the example of S/N ratio in first experiment trails in TIG welding process parameters and responses. As can be observed from the variable S/N ratio in TABLE 5, each TIG welding process parameter has an impact on the mechanical qualities of the weld joint. This trend in S/N ratio variation clearly shows that, in comparison to other process parameters (Gas flow rate and filler rod diameter), the input current is the process parameter that influences the weld joint's mechanical property the most. This trend is evidenced from Figs 6-8.

$$S / N = -10 \log_{10} \left(\frac{1}{n} \sum_{i=1}^{n} \frac{1}{Y_i^2} \right) \quad (1)$$

Where
N – the number of experiment results, $n = 2$ and
y – corresponding tensile and hardness values of each trails.

TABLE 5

Enumerates the values of ANOVA analysis for the S/N ratios

S. No	Source	dF	Seq SS	Adj SS	Adj MS	P
1	Current	2	0.5634	0.5634	0.28168	41.5%
2	Gas flow rate	2	0.1276	0.1276	0.06378	12.5%
3	Fill rod diameter	2	4.1996	4.1996	2.0998	37.5%
4	Residual Error	2	0.4553	0.4553	0.22765	8.50%
5	Total	8	5.3458	—	—	—

Taking first trial,

$$= -10 \log_{10} [1/2 \times ((1/286.152) + (1/862))] = \\ = 41.32 \text{ dB} \quad (2)$$

Based on input and out responses of TIG welding process, develop the ANOVA and linear regression mathematical equations. MINITAB 17 was used to create a multiple linear regression model based on the experimental results. The regression analysis equations are listed below.

The output response regression equations are accordingly,

$$\text{Tensile strength (MPa)} = 155 - 170 \text{ Current} \\ - 10 \text{ Gas flow} - 2.4 \text{ Filler rod diameter} \quad (3)$$

$$\text{Hardness (HV)} = 77.1 - 170 \text{ Current} \\ - 10 \text{ Gas flow} - 2.4 \text{ Filler rod diameter} \quad (4)$$

$$\text{Impact strength (J)} = 12.4 - 170 \text{ Current} \\ - 10 \text{ Gas flow rate} - 2.4 \text{ Filler rod diameter} \quad (5)$$

Percentage contribution (P) can be used to evaluate the significance of change in the process parameters on the quality characteristics

Calculation for percentage contribution:
Percentage contribution (P) = (SS'A / SST) × 100
Current (A) = 2.2185/5.3458 × 100 = 41.5%
Gas Flow Rate (lpm) = 0.6682/5.3458 × 100 = 12.5%
Filler Rod Diameter (mm) = 2.0046/5.3458 × 100 = 37.5%
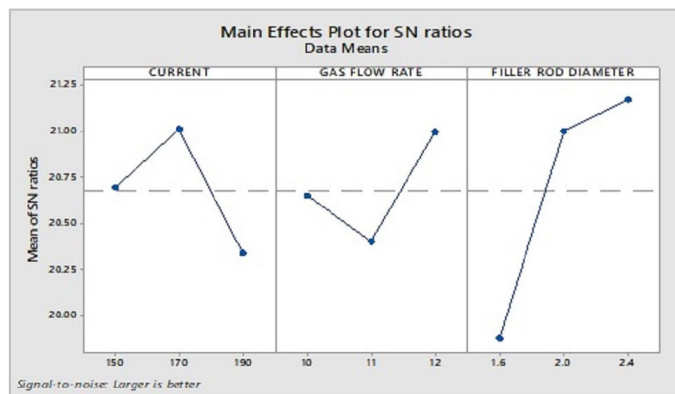Error (E) = 0.4553/5.3458 × 100 = 8.5%

Fig. 8. Effects of process parameters on S/N ratios for Impact resistance

4.2. TIG welding of AA5083-H111 andAA5052-H32 under optimized process parameters

As indicated by the results above, the process parameter values that affect the weld joint mechanically were obtained and it was established that the welding current of the TIG welding process is the most contributing factor in improving the joint`s mechanical integrity. As such, the optimized process parameters were used to TIG weld the AA5052 and AA5083 dissimilar metals and the resulting weld joint shown in Fig. 9a was analyzed for its joint composition and metallographic characteristics. Aluminium plates of 5 mm thicknessnamely (AA5052 and AA5083) were TIG welded under 170 A of constant current using industry standard ER 5356 filler rods.

TABLE 6 illustrates the chemical composition of the TIG welded joint under optimal process conditions. The macrostructure of the improved TIG welded connection is shown in Fig. 9(b). The welded joints were then further subjected to metallographic characterization under optical microscopy, SEM analysis to observe the grain structure and the microstructural distribution of the joint.

4.3. Microscopic analysis

The optimized TIG welded joints were analyzed under optical microscope for characterization of the joint for identifying grain boundaries, metal phase distribution and boundaries in the
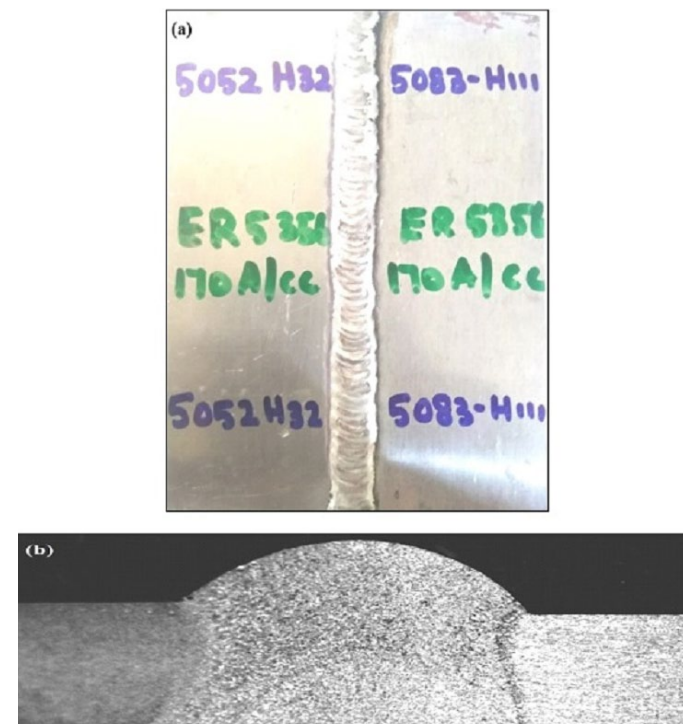

Fig. 9. (a) TIG welded AA5052-H32 – AA5083-H111 under optimized process parameters (b) Macrostructure of the TIG welded joint

weld joint. The microstructural imagery obtained is shown in Fig. 9. The investigations were done at magnification level of 100× for the base metals AA5052-H32 and AA5083-H111 and the welded joint were also inspected at 100× respectively. The microstructures of the base metals highlight the variance in the structural composition between the dissimilar metals. The presence of even distribution of grains is observed in the weld joint. Fig. 10(a,b) shows the microstructure of AA5052-H32 and AA5083-H111 base metal at 100× magnification. Similarly, Fig. 10(c) shows the microstructure at the core of the weld region of S9 sample at 100× magnification. The S9 sample which posses' least mechanical properties which were shown in Fig. 5. In Fig. 10(d) the microstructure at the core of the weld region of optimized sample (S-10) at 100× magnification. The properties of the optimized sample are shown in TABLE 7 respectively. From the Fig. 10c it is clearly evident that the grains at the center of the weld are coarser for the S4 sample (sample with least strength). On the contrary, for the optimized weld sample

TABLE 6

Chemical composition of the TIG welded joints

S. No	Sample	Al	Mg	Mn	Fe	Si	Cr	Cu	Zn	Ti
1	170A/CC/ER5356 (optimized Sample S-10)	Bal	4.9	0.114	0.183	0.159	0097	0.012	0.018	0.065

TABLE 7

Mechanical properties of the Optimized sample (S-10)

S. No	Sample Number	Current	Gas Flow Rate	Filler Rod Diameter	Ultimate tensile strength (MPa)	Vickers Hardness	Impact strength	Elongation
1	Optimized Sample (S-10)	170	10	2.4	161.2	79	12.5	12.25

(a) AA5052-H32 -100X

(b) AA5083-H111- 100X

(c)Microstructure of S4 sample (100X)

(d) Microstructure of optimized sample (S-10) (100X)

(e) SEM Microstructure of S4 (1000X)
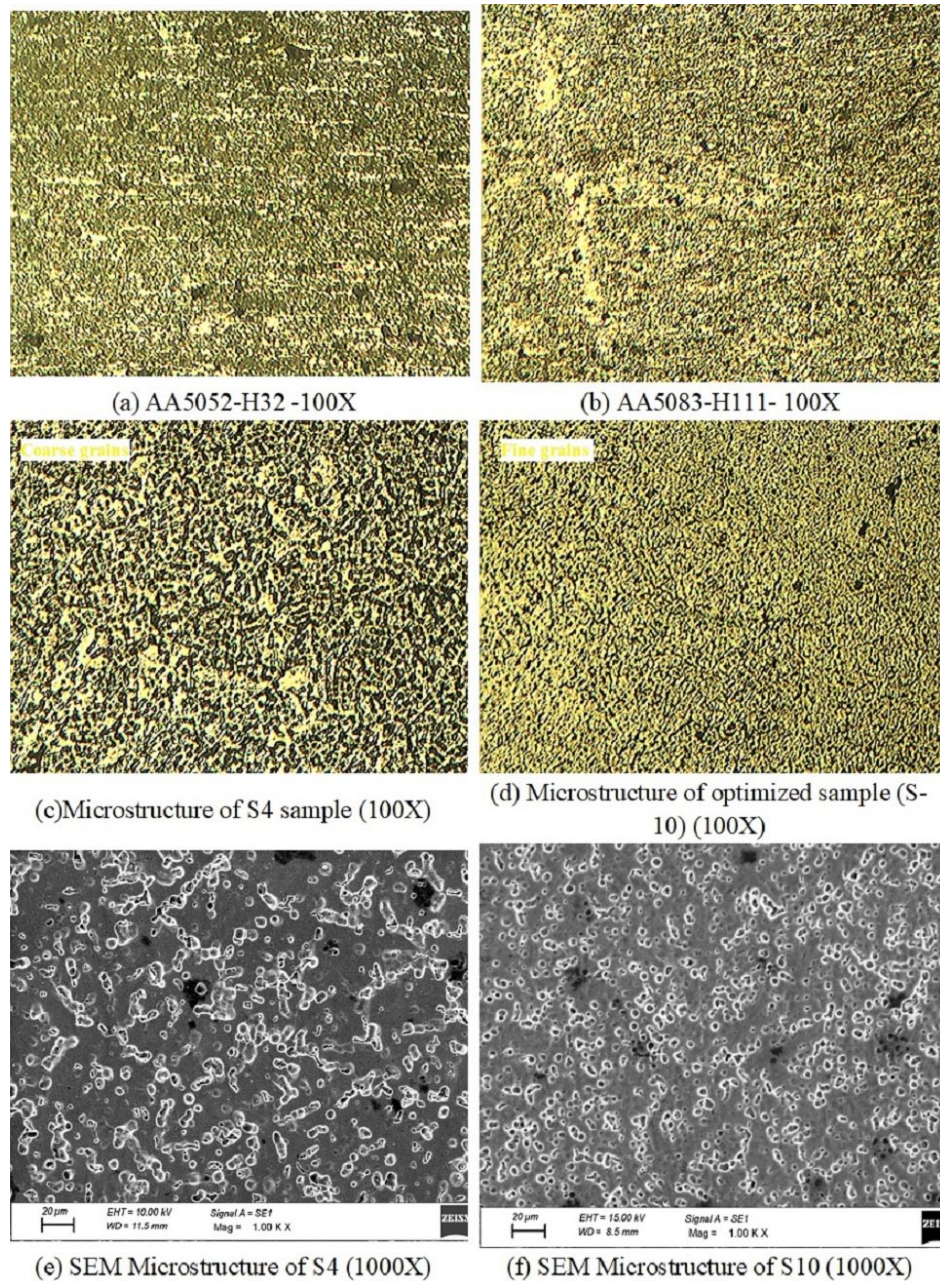
(f) SEM Microstructure of S10 (1000X)

Fig. 10. Microstructural analyses of welded joints

(S10), finer grains at the center of the weld zone are seen. According to Hall-Petch relation fine grain results in enhanced mechanical properties which were evident [16,17]. This justifies that enhanced mechanical properties of the joint. Further the SEM microstructures also reinforces with evidence that the fine grains are seen at the weld zone for the optimized welded joint compared to the S4 joint which coarse grains. The images are shown in Fig. 10(f) and Fig. 10(e) respectively. The FZ consist of cast grains which are coarse and also possibility of existence of the weld defects resulting as the crack initiation site at the FZ. From the literatures The possibly of presence of Mg2Si and Al6 (Fe, Mn) hard precipitates at FZ by welding with Al-Mg Filler rod increases the hardness at the FZ compared to 5052 BM. Hence even though the hardness is higher at FZ of weld it is also the fracture location.

5. Conclusion

The process parameters that affect the TIG welded joint of the dissimilar base metals AA5052-H32 and AA5083-H111 was performed using Taguchi method followed by Analysis of Variance. The optimized values for the process parameters: Input constant Current, Gas Flow Rate, Filler Rod Diameter were obtained as a result. Among the process parameters, the input current (41.5% of contribution) was shown to have the greatest impact on improving the mechanical (161.2 MPa for ultimate strength) qualities of the weld joint. The TIG weld was performed using optimized input constant current value to obtain the optimized TIG welded specimen. The mechanical properties of the process parameter optimized TIG welded dissimilar aluminium alloy were examined alongside the base metals using a variety

of tests, including ultimate tensile strength, microhardness, Fractographic behavior, and impact resistance analysis. The tensile tests revealed joint efficiency for UTS at 78.89%. As a result, the new technology in metal joining processes mentioned in this study can improve metal hardness and tensile strength. According to contemporary welding research, the Taguchi approach is an excellent tool for welding process improvement. In future the studies can be elaborated for L27 samples. Further other factors such as voltage which are influencing the weld joint strength might also be analyzed. Latest optimization techniques can be adopted.

REFERENCES

[1] A.P. Dhanaraj, S. Kumarasamy, Mechanical properties and metallurgical characterization of FSPed TIG and TIG welded AA5052-H32/AA5083-H111 dissimilar aluminium alloys, Metall. Res. Technol. **118** (3), 304 (2021).

[2] H.S. Grover, V. Chawla, G.S. Brar, Comparing mechanical and corrosion behaviour of TIG & FSW weldments of AA5083-H321, Indian. J. Sci. Technol. **10** (45), 1-8 (2017).

[3] Y.S Tarng, H.L. Tsai, S.S. Yeh, Modelling, Optimization and Classification of Weld Quality in Tungsten Inert Gas Welding, Int. J. Mach. Tools Manuf. **39** (9), 1427-1438H (1999).

[4] A. Khalid, A. Lateef, M. Javed, T. Pramesh, Influence of welding speed on tensile strength of welded joint in TIG welding process,, Int. J Appl. Eng. Res. **1** (3), 518 (2010).

[5] K. Vasu, H. Chelladurai, Addanki Ramaswamy, S. Malarvizhi, V. Balasubramanian, Effect of fusion welding processes on tensile properties of armor grade, high thickness, non-heat treatable aluminium alloy joints, Def. Tech. **15** (3), 353-362 (2019).

[6] Bo Wang, Song-bai Xue, Chao-li Ma, Yi-long Han, Zhong-qian Lin, Effect of combinative addition of Ti and Sr on modification of AA4043 welding wire and mechanical properties of AA6082 welded by TIG welding, Trans. Nonferrous Met. Soc. China **27**, 272-281 (2017).

[7] A. Farzadi, S. Serajzadeh, A.H. Kokabi, Modelling of Heat Transfer and Fluid Flow during Gas Tungsten Arc Welding of Commercial Pure Aluminium, Int. J. Adv. Manuf. Technol. **38** (3), 258-267 (2008).

[8] Y. Liu, W. Wang, J. Xie, S. Sun, L. Wang, Y. Qian, Y. Wei, Microstructure and mechanical properties of aluminum 5083 weldments by gas tungsten arc and gas metal arc welding, Mater. Sci. Eng. A. **549**, 7-13 (2012).

[9] M.P. Bharani Dharam, T. Gowtham, H.S. Rahmanudeen, M. Adam Khan, S. Jani, G. Suganya Priyadharshini, Mechanical and electrochemical behaviour of austenitic stainless steel and nickel-based alloy dissimilar joint. In Proceedings of the international conference on surface engineering. 9-11, (2018).
https://inis.iaea.org/search/search.aspx?orig_q=RN:52080804

[10] C. Rajendran, K. Srinivasan, V. Balasubramanian, H. Balaji, P. Selvaraj, Feasibility study of FSW, LBW and TIG joining process to fabricate light combat aircraft structure, Int. J. Lightweight Mater. Manuf. **4** (4), 480-490 (2021).

[11] C.A. Anoop, P. Kumar, Application of Taguchi Methods and ANOVA in GTAW Process Parameters Optimization for Aluminium Alloy 7039, Int. J. Eng. Inn. Tech. **2** (11), 54-58 (2013).

[12] V. Chaudhary, A. Bharti, Azam, S.M. Kumar, K.K. Saxena, A re-investigation: Effect of TIG welding parameters on microstructure, mechanical, corrosion properties of welded joints, Mater. Today:. Proc. **45**, 4575-4580 (2021).

[13] K. Kishore, P.V. Gopal Krishna, K. Veladri, G.K. Kumar, Analysis of defects in gas shielded arc welding of AA 6351 using Taguchi methods, Int. J. Ap. Eng. Res. **5** (3), 393-399 (2010).

[14] Husain Mehdi, R.S. Mishra, Investigation of mechanical properties and heat transfer of welded joint of AA6061 and AA7075 using TIG+FSP welding approach, J. Adv. Joining Processes **1**, 100003 (2020).

[15] S.P. Jani, A.S. Kumar, M.A. Khan, A.S. Jose, Design and optimization of unit production cost for AWJ process on machining hybrid natural fibre composite material, Int. J. Lightweight Mater. Manuf. **4** (4), 491-497 (2021).

[16] E.O. Hall, The deformation and ageing of mild steel: III discussion of results, Proc. Phys. Soc. London, Sect. B **64** (9), 747 (1951).

[17] N.J. Petch, The cleavage strength of polycrystals, J. Iron. St. Inst. **174**, 25-28 (1953).